Functional Materials 14, No.4 (2007)

Back surface reflector optimization for thin single crystalline silicon solar cells

V.R.Kopach, M.V.Kirichenko, S.V.Shramko, R.V.Zaitsev, I.T.Tymchuk*, V.A.Antonova*, A.M.Listratenko*

National Technical University "Kharkiv Polytechnical Institute", 21 Frunze St., 61002 Kharkiv, Ukraine
*State Enterprise "Scientific and Research Technological Institute of Instrument Engineering", 40/42 Primakov St., 61010 Kharkiv, Ukraine

Received October 12, 2007

It has been shown that for single crystalline silicon solar cells (Si–SC) with 180–200 μm thick base crystals, the optimum back surface reflector (BSR) is TiO_2/Al with 0.18 μm thick oxide layer. At such BSR, the reflection coefficient for photoelectric active sunlight reaching the back surface of Si–SC at 0.88–1.11 μm wavelengths attains 81 to 92 % against of 71 to 87 % at direct Al contact with back surface of silicon base crystal.

Показано, что для монокристаллических кремниевых фотоэлектрических преобразователей (Si-ФЭП) солнечной энергии с толщиной базовых кристаллов 180÷200 мкм наиболее оптимальным является тыльно-поверхностный рефлектор TiO_2/Al с толщиной оксидного слоя 0,18 мкм. Коэффициент отражения фотоэлектрически активного солнечного излучения указанным рефлектором, достигающего тыльной поверхности таких Si-ФЭП при длинах волн 0,88÷1,11 мкм, составляет 81÷92 % в отличие от 71÷87 % при непосредственном контакте Al с тыльной поверхностью базового кристалла кремния.

At present, solar batteries based on solar cells (SC) are the main electric power sources for the most spacecrafts [1–3]. The priority development way to new design-technological solutions (DTS) which are capable to ensure the highest efficiency and mass-power performances P_M of single crystalline Si–SC with enhanced radiation resistance at use of an available technological infrastructure is decreasing of silicon base crystal (Si–BC) thickness t and sunlight energy losses in Si–BC bulk, as well as on base crystals front and back surfaces [4, 5].

At the stage of design improvement on Si–SC with horizontal n^+-p-p^+ diode structure, we have found the optimal ways to Si–BC thinning down to t<200 μm as well as to formation of n^+- and p^+- diffusion layers [4]. Researches and development of the technology which will provide the optimum geometry of Si–BC photoreceiving surface structure shaped as inverted pyramids are in progress [5] that are necessary for an essential reduction of light reflection coefficient R by the specified surface. At the same time, Si–SC with t<200 μm show essential losses of solar energy due mainly to reduced photoactive volume of semiconductor material at direct radiation passage through Si–BC before interaction with one of electrodes [4] where the photoelectic active component of sunlight can be absorbed with heat release. As it was shown before [6], a radical way to the loss reduction is to provide a sunlight reflector on the side of the back surface consisting of two-layer structure SiO_2/Al. However, in corresponding information sources, there are no data on

SiO_2 oxide layer optimum thickness l_{OX}^{opt} in such structure. At the same time, that oxide seems to be not optimum for every Si–SC DTS; moreover, the above-mentioned bilayer structure has a principal drawback caused by its thermodynamic instability because of aluminum ability to active reduction of SiO_2 [7] that should result in R reduction during active life of Si–SC with this kind of back surface reflector. Therefore, the purpose of this work was to determine the optimum design of the back surface sunlight reflector with the transparent oxide (TO)/Al bilayer structure for efficiency and active lifetime improvement of single crystal Si–SC with horizontal rectifying junction.

The growing of good quality SiO_2 layer for the reflector under consideration with thickness over several tens nanometers requires a high-temperature oxidation of the silicon crystal surface. To that process, temperatures from 800 up to 1200°C [8–10] are necessary as a rule, that is fraught with undesirable changes in concentration profiles of n^+- and p^+- diffusion layers formed before at 900–1000°C [11]. At the same time, during the development and manufacture of the single crystal Si–SC with horizontal n^+-p-n^+ diode structure, a low-temperature manufacturing method of the transparent oxide TiO_2 layer coating was developed [11, 12], which is used as anti-reflection coating from the side of the Si–BC frontal surface. Between TiO_2 and n^+-Si layer, an about 10 nm thick SiO_2 layer might be places which is formed at a temperature not exceeding 200°C and intended for n^+-Si passivation [12]. With reference to the back surface reflector design, that circumstance allows to consider the TiO_2 layer made according to the low-temperature process as a prospective alternative to SiO_2 layer made using the high-temperature process. The arrangement of a thin (about 10 nm) SiO_2 passivation layer between TiO_2 and p^+-Si from the side of Si–BC back surface formed at temperature not higher than 200°C is obviously expedient, too.

According to [13], the optimum oxide thickness l_{OX}^{opt} for bilayer TO/metal reflector to provide the reflection maximum at the chosen wavelength λ can be calculated as

$$l_{OX}^{opt} = \frac{2\pi m + \arg r_2}{4\pi n_{OX}}\lambda, \quad (1)$$

where

$$arg\ r_2 = \mathrm{arctg}\left(\frac{2n_{OX}k_M}{n_{OX}^2 - n_M^2 - k_M^2}\right), \quad (2)$$

$n_{OX} = n_{OX}(\lambda)$ is the refraction coefficient of oxide dielectric layer; $n_M = n_M(\lambda)$ and $k_M = k_M(\lambda)$ are refraction and extinction coefficients of metal, respectively; $m = 1, 2, 3, \ldots$.

In the case of oxide dielectric layer of interferential thickness between silicon and metal, when t exceeds considerably λ of the radiation incident from the side of Si–SC frontal surface, the expression for $R(\lambda)$ looks like

$$R = 1 - \frac{(1 - |f_0|^2)(1 - |r_1|^2)}{1 - |f_0|^2|r_1|^2}. \quad (3)$$

where

$$f_0 = \frac{n_0 - n_{Si}}{n_0 + n_{Si}}. \quad (4)$$

$$|r_1|^2 = \frac{|f_1|^2 + |r_2|^2 + 2|f_1||r_2|\cos(n_{OX}l_{OX}^{opt}4\pi/\lambda - \arg r_2)}{1 + |f_1|^2|r_2|^2 + 2|f_1||r_2|\cos(n_{OX}l_{OX}^{opt}4\pi/\lambda - \arg r_2)}, \quad (5)$$

$$f_1 = \frac{n_{Si} - n_{OX}}{n_{Si} + n_{OX}}. \quad (6)$$

$$|r_2| = \left[\frac{(n_{OX} - n_M)^2 + k_M^2}{(n_{OX} + n_M)^2 + k_M^2}\right]^{1/2}, \quad (7)$$

$n_0 = n_0(\lambda)$ is the refraction coefficient of environment (air or covering glass) with which the Si–SC front surface is in contact; $n_{Si} = n_{Si}(\lambda)$ is the Si–BC refraction coefficient.

It is obvious that calculation of l_{OX}^{opt} and $R(\lambda)$ values is expedient with reference to SC in the case when t is smaller than depth $X_{100}(\lambda)$ for full (100 %) light absorption at the set λ value. On the other hand, efficiency, P_M and longevity of a SC with horizontal diode structure n^+-p-p^+ or p^+-n-n^+ type increases at reduction of the t/L ratio, where L is the diffusion length of minority charge carriers in Si–BC of p- or n- type, respectively [14]. Therefore, a range of λ values for which calculation of l_{OX}^{opt} and $R(\lambda)$ is expedient should be limited from the side of longer waves by the red edge of an internal photoelectric effect in Si–BC corresponding to $\lambda_{max}\approx 1.11$ μm [13], and from the side of shorter waves, by the value λ_{min} at which the following conditions are simultaneously satisfied:

$$t/L < 1, \quad (8)$$

$$t < X_{100}(\lambda_{\min}), \quad (9)$$

$$R(\lambda_{\min}) \div R(\lambda_{\max}) \geq 0.8. \quad (10)$$

According to [14],

$$L_{n,p} = \left(\frac{kT\mu_{n,p}\tau_{n,p}}{e}\right)^{1/2}, \quad (11)$$

where k is the Boltzmann constant; T, temperature; e, charge of electron; $\mu_{n,p}$ and $\tau_{n,p}$, mobility and lifetime of minority charge carriers in Si–BC, respectively.

In [15], we have shown results of the first performed researches of τ_n and L_n values for electrons in domestic SC based on p-type Si–BC, with specific resistance 10 Ω·cm and mobility $\mu_n \approx 1200$ cm^2/(V·s). The τ_n values determined from the dependence of SC open circuit voltage drop on time after illumination cutoff and L_n values calculated from those for such SC with t = 190±10 μm, textured front surface and optimized manufacturing conditions of n^+-p-p^+ diode structure were 53–74 μs and 408–483 μm, respectively. The subsequent refinement of the mentioned parameters of minority charge carriers carried out by us for the same Si–SC taking into account the n^+-p homojunction capacity influence on experimental dependence of SC open circuit voltage U_{OC} drop on time τ after illumination cutoff, and also by use of the advanced method [16] for analytical processing of the $U_{OC} = U_{OC}(\tau)$ dependences, has shown, that more realistic values are $20 \leq \tau_n \leq 26$ μs and $250 \leq L_n \leq 286$ μm. It follows therefrom that taking into account the expression (8) and nearest prospects of technological possibilities evolution for domestic single crystalline Si–SC production [4, 15] it is just t = 180 μm appropriate to calculation of l_{OX}^{opt} and $R(\lambda)$ values.

Taking into account expression (9), it is possible to determine λ_{min} value from dependence of depth corresponding to absorption of 99.995 % of light quanta total amount (which practically corresponds to the parameter X_{100} entered above) on λ in an interval (λ; λ+dλ) as follows. According to [17], the expression describing light absorption in Si–BC looks as

$$N_X(\lambda) = N_0(\lambda)\exp[-\frac{X}{X_{63}(\lambda)}], \quad (12)$$

where N_X is the density of photon flow passing into Si–BC from the side of its front surface up to depth X; N_0, density of photon flow crossing the Si–BC front surface; X_{63}, classical value of light absorption depth corresponding to absorption of approximately 63 % of the photons which have crossed the Si–BC frontal surface ($X_{63} = \alpha^{-1}$, $\alpha = 4\pi k/\lambda$, k, extinction coefficient [17]).

If $N_X(\lambda)$ value in (12) is assumed to be $0.00005 \cdot N_0(\lambda)$, it is easy to show that after the natural logarithm of expression (12) is found it is possible to get the following expression for X_{100} calculation: $X_{100} = -X_{63} \cdot \ln 0.00005$. It is obvious that, for example, the expression for X_{90} calculation can be obtained in similar way, which has the form $X_{90} = -X_{63} \cdot \ln 0.1$. Since the spectral dependence $X_{63}(\lambda)$ for silicon single crystal is well-known [17], it is easy to calculate $X_{90}(\lambda)$ and $X_{100}(\lambda)$ using these expressions.

Since t for domestic Si–SC for space applications being now in development approaches 180 μm, therefore, the X_{63}, X_{90} and X_{100} values are to be determined with reference to t = 180 μm. This allows to limit in zero approximation the wavelength range of photoactive radiation being of interest as $0.8 < \lambda \leq 1.1$ μm [17].

That wavelengths range was defined more precisely using the above-mentioned $X_{63}(\lambda)$, $X_{90}(\lambda)$ and $X_{100}(\lambda)$ dependences, that were plotted using numerical values of $X_{63}(\lambda)$ from [17], as well as $X_{90}(\lambda)$ and $X_{100}(\lambda)$ calculated based on those. In Fig. 1, the $X_{63}(\lambda)$, $X_{90}(\lambda)$ and $X_{100}(\lambda)$ dependences are presented in semi-logarithmic coordinates (lg$X$; λ). The lower limit of photoactive radiation range being of interest was determined using the $X_{100}(\lambda)$ curve at a sufficient accuracy as follows. In Fig. 1, a straight line parallel an abscissas axis corresponding to function $\lg[X(\lambda)]_{X=t} = const$ (where for considered SC t = 180 μm as noted above) was drawn. In this case, lg180 = 2.26. That operation allows to determine the limiting wavelength value at which the photoelectric active absorption of radiation practically completely ceases at direct passing through 180 μm thick silicon crystal. It is obvious that the required wavelength corresponds to abscissa of the intersection point of the function lg $[X(\lambda)]_{X=t} = const$ with the function $X_{100}(\lambda)$. As to the wavelength range of interest, the required wavelength has the sense of λ_{min}. As is obvious from Fig. 1, $\lambda_{min} \approx 0.88$ μm in the considered case. Thus, the wavelength range of the photoactive radiation being of interest from the viewpoint of l_{OX}^{opt} and $R(\lambda)$ calculation as well as for determination of optimum SiO_2 and TiO_2 thickness $l_{OX}^{opt,\max}$ for back surface reflectors SiO_2/Al and TiO_2/Al (providing their maximal integrated reflectivity in the set wavelength range), is $0.88 \le \lambda \le 1.11$ μm. It is to note that using the procedures similar to that described for determination λ_{min} for practically complete absorption of photoactive radiation, it is easy to determine λ_{min} for absorption of 90 % and 63 % of photoactive radiation. As is obvious from Fig. 1, these values approximately are 0.99 μm and 0.96 μm, respectively.

As follows from the above, the main study objects were layered Si/SiO_2/Al and Si/TiO_2/Al structures with oxide layers of interferential thickness. At the same time, to illustrate the contribution from those oxide layers into the enhanced back surface reflector reflectivity, the $R(\lambda)$ were calculated for the case of oxide layer absence between Si and Al, i.e. for structure Si/Al, when $l_{OX} = 0$. According to [13], the $|r_1|^2$ value in expression (3) for $R(\lambda)$ was assumed to be

$$|r_1|^2 = \frac{(n_{Si} - n_M)^2 + k_M^2}{(n_{Si} + n_M)^2 + k_M^2}.$$

The $l_{OX}^{opt}(\lambda)$ and $R(\lambda)$ values were calculated using expressions (1) and (3) basing on the Excel 2003 software. The f_0 value was defined both for the case of SC front surface contacting with air and under account for the SC front surface protection by covering glass of not-interference thickness glued to the crystal by silicon rubber with optical properties similar to protecting glass [17]. For the specified reason, the n_0 value in the expression (4) was assumed to be 1.0 in the first case and 1.5 (by analogy with [13, 17]) in the second one. The m value in the expression (1) was adopted to be 1. The spectral dependences $n_{Si}(\lambda)$, $n_{OX}(\lambda)$, $n_M(\lambda)$ and $k_M(\lambda)$ required to calculate the $l_{OX}^{opt}(\lambda)$

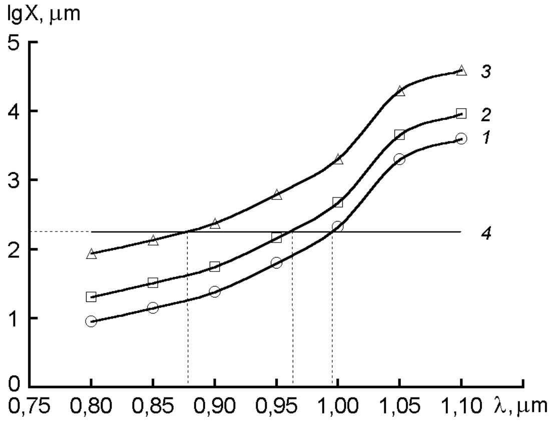

Fig. 1. lg$X(\lambda)$ dependences for the radiation absorption in silicon single crystal at absorption degree of 63 % (X_{63}, curve *1*), 90 % (X_{90}, curve *2*) and essentially complete (X_{100}, curve *3*) as well as the lg $[X(\lambda)]_{X=t} = const$ function at t = 180 μm (curve *4*).

and $R(\lambda)$ values were taken from the sources: $n_{Si}(\lambda)$ from [18], $n_{SiO_2}(\lambda)$ from [19], $n_{TiO2}(\lambda)$ from [20, 21], $n_{Al}(\lambda)$ and $k_{Al}(\lambda)$ from [22, 23].

The dependences $l_{OX}^{opt}(\lambda)$ and $R[(\lambda), l_{OX}^{opt}(\lambda)]$ at $n_0 = 1.0$ and $n_0 = 1.5$ for back surface reflector SiO_2/Al are plotted in Fig. 2, a–c, and for back surface reflector TiO_2/Al, in Fig. 3, a–c. The $R(\lambda)$ plots at $n_0 = 1.0$ and $n_0 = 1.5$ in case l_{OX}=0 are presented in Figs. 2b, c and 3b, c, respectively. As seen from Figs. 2b, c and 3b, c, the substitution of Al back surface reflector by SiO_2/Al and TiO_2/Al ones provides an essential increase of the reflectivity as compared to that of Al in $\lambda > 0.8$ μm range at specified values l_{OX}^{opt}.

Consideration of the all $R[\lambda l_{OX}^{opt}(\lambda),\ n_0]$ curves presented in Figs. 2 and 3 shows that both at $n_0 = 1.0$ and at $n_0 = 1.5$, the optimal thickness $l_{OX}^{opt,\max}$ values of SiO_2 and TiO_2 providing the maximal integrated reflectivity of SiO_2/Al and TiO_2/Al back surface reflectors in the preset wavelength range, according to criterion (10), are:

$$l_{OX}^{opt,\max} = 0.32\ \mu m \text{ for } SiO_2/Al;$$
$$l_{OX}^{opt,\max} = 0.18\ \mu m \text{ for } TiO_2/Al.$$

The advantages of such reflectors in $R(\lambda)$ as compared to $R(\lambda)$ for Al reflector are seen most clearly in Fig. 4 and in Table. Besides, the oxide interlayer between silicon and aluminum hinders the degradation of the re-

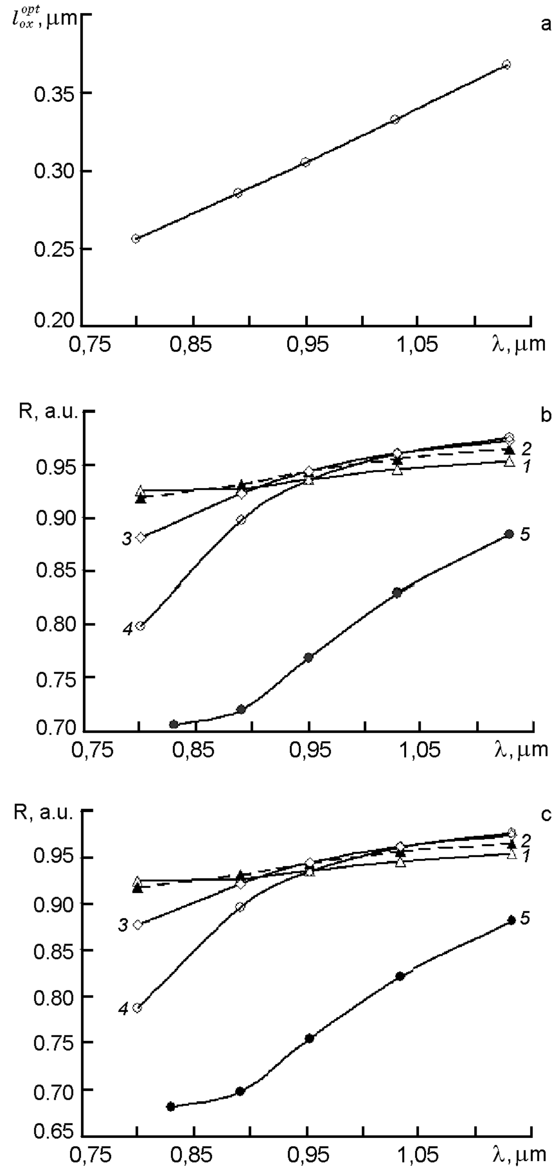

Fig. 2. Calculated dependences for SiO_2/Al back surface reflector: $l_{OX}^{opt}(\lambda)$ (a); $R(\lambda)$ for l_{OX}^{opt} (μm): 0.26 (λ_1 = 0.8 μm) (*1*); 0.29 (λ_2 = 0.9 μm) (*2*); 0.32 (λ_3 = 1.0 μm) (*3*); 0.35 (λ_4 = 1.1 μm) (*4*); l_{OX} = 0 (*5*) at n_0 = 1.0 (b) and n_0 = 1.5 (c).

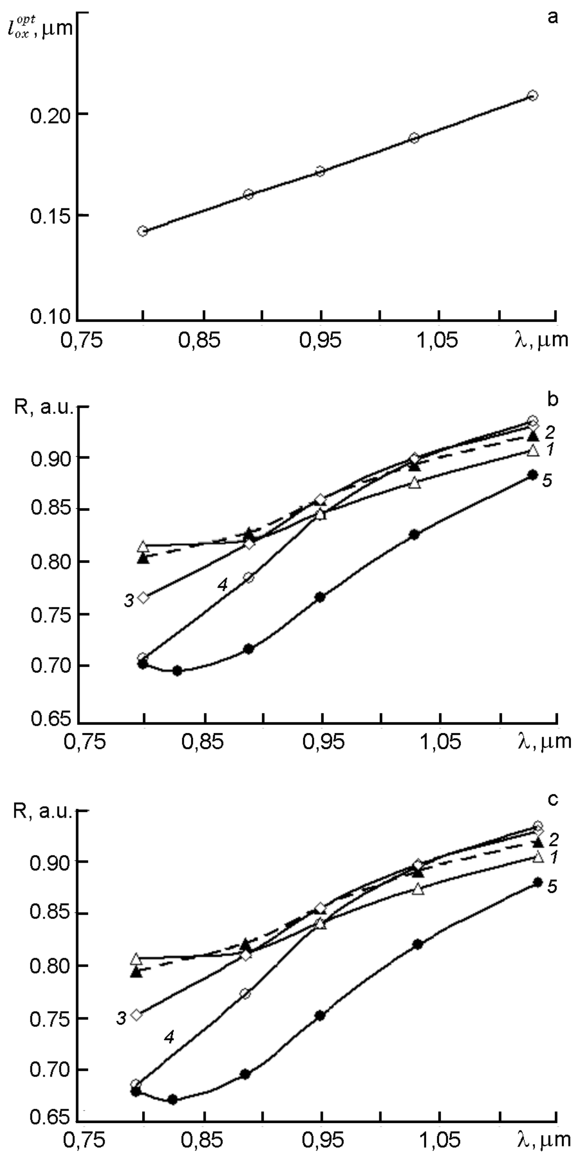

Fig. 3. Calculated dependences for TiO_2/Al back surface reflector: $l_{OX}^{opt}(\lambda)$ (a); $R(\lambda)$ for l_{OX}^{opt} (μm): 0.14 (λ_1 = 0.8 μm) (*1*); 0.16 (λ_2 = 0.9 μm) (*2*); 0.18 (λ_3 = 1.0 μm) (*3*); 0.20 (λ_4 = 1.1 μm) (*4*); l_{OX} = 0 (*5*) at n_0 = 1.0 (b) and n_0 = 1.5 (c).

flector optical properties and ensures lowering of surface recombination on the Si–BC back surface [6]. As is seen in Figure 4 and Table, it is just the SiO_2/Al back surface reflector that provides the highest integrated reflectivity in the $0.88 \le \lambda \le 1.11$ μm wavelength range. However, according to the analysis carried out before, in conditions of domestic single crystal Si–SC production for domestic single crystal Si–SC now under development with base crystal thickness of 180 to 200 μm, optimum is rather the TiO_2/Al back surface reflector with the $l_{OX}^{opt,\max}$ value mentioned above.

Thus, basing on the actuality of high-efficiency and long-lived domestic single crystal Si–SC development with base crystal thickness t = 180 to 200 μm, the spectral dependences of oxide layer optimum thickness $l_{OX}^{opt,\max}$ of SiO_2/Al and TiO_2/Al back surface reflectors for such Si–SC as well as the spectral

Table. $R(\lambda)$ values for the investigated back surface reflectors with the optimum thickness of transparent oxides in the wavelength range $0.88 \le \lambda \le 1.11$ μm

Reflector	Al	SiO_2/Al	TiO_2/Al
$l_{OX}^{opt,\max}$, μm	0.00	0.32	0.18
$n_0 = 1.0$, $R(0.88) \div R(1.11)$, %	71.4÷86.8	91.9÷97.0	81.3÷92.3
$n_0 = 1.5$, $R(0.88) \div R(1.11)$, %	68.9÷86.2	91.6÷97.0	80.1÷92.1

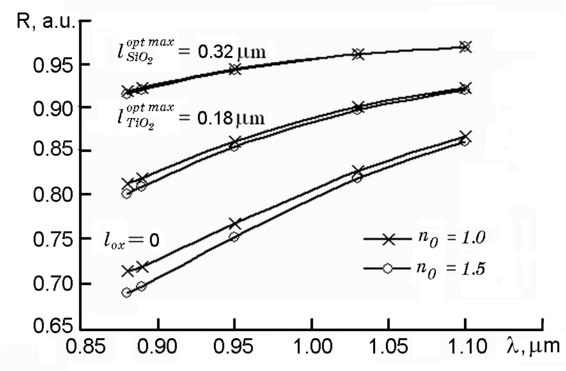

Fig. 4. $R(\lambda)$ dependences for SiO_2/Al and TiO_2/Al back surface reflectors with $l_{OX}^{opt} = l_{OX}^{opt,\max}$ as well as for Al reflector ($l_{OX} = 0$) at $n_0 = 1.0$ and $n_0 = 1.5$.

dependences of reflection coefficient $R(\lambda)$ at various l_{OX}^{opt} and refraction coefficients n_0 of environment (air or covering glass at the front surface of Si–SC contacts) for $0.88 \le \lambda \le 1.11$ μm were calculated using the Excel 2003 software taking into account the key expressions (1) and (3). The limits of λ range are defined by the smaller t value mentioned above and the band gap width of crystalline silicon. The optimum thickness $l_{OX}^{opt,\max}$ of SiO_2 and TiO_2 layers providing the maximal integrated reflectivity of considered reflectors in the whole specified λ range have been determined from calculated dependences R[λ, $l_{OX}^{opt}(\lambda)$,n_0] taking into account the criterion $R(\lambda) \ge 0.8$. It is shown that in conditions of domestic Si–SC production, the optimum back surface reflector is TiO_2/Al with $l_{OX}^{opt,\max} = 0.18$ μm.

References

1. P.Iles, in: Proc. 2nd World Conf. and Exhibit. on Photovoltaic Solar Energy Conversion, July 6–10, Vienna, Austria (1998), p.67.
2. S.Bailey, H.Curtis, G.Landis et al., in: Proc. 17th Europ. Photovoltaic Solar Energy Conf., Oct 22–26, Munich, Germany (2001), p.2137.
3. A.Goetzberger, in: Proc. 17th Europ. Photovoltaic Solar Energy Conf., Oct. 22–26, Munich, Germany (2001), p.9.
4. V.A.Antonova, V.N.Borshchov, V.R.Kopach et al., *Radiotekhnika*, No.139, 113 (2004).
5. M.V.Kirichenko, I.T.Tymchuk, V.A.Antonova et al., *Functional Materials*, **14**, 61 (2007).
6. M.A.Green, J.Zhao, A.Wang et al., *Solar Energy Mater. Solar Cells*, **65**, 9 (2001).
7. A.E.Gershinskii, A.A.Khoromenko, F.L.Edelman, *Phys. Stat. Sol. A*, **25**, 645 (1974).
8. N.A.Kolobov, M.M.Samohvalov, Diffusion and Oxidization of Semiconductors, Metallurgia, Moscow (1975) [in Russian].
9. Y.C.Cheng, Modern Probl. Surface Phys.: 1st Int. Sch. "Condensed Matter Phys., Varna, Sept.29–Oct.12, 1980, Lect.", Sofia (1981), p.620.
10. M.Itsumi, F.Kiyosumi, *Appl. Phys. Lett.*, **40**, 496 (1982).
11. A.M.Listratenko, *Radiotekhnika*, No.121, 121 (2001).
12. V.A.Antonova, V.N.Borshchov, V.R.Kopach et al., *Functional Materials*, **10**, 168 (2003).
13. M.M.Koltun, Selective Optical Surfaces of Solar Energy Converters, Nauka, Moscow (1979) [in Russian].
14. A.L.Fahrenbruch, R.H.Bube, Fundamentals of Solar Cells. Photovoltaic Solar Energy Conversion, Academic Press, New York (1983).
15. M.V.Kirichenko, R.V.Zaitsev, N.V.Deyneko et al., *Radiofizika i Elektronika*, **12**, 255 (2007).
16. J.E.Mahan, T.W.Ekstedt, R.I.Frank et al., *IEEE Trans. Electron Devices*, **ED-26**, 733 (1979).
17. M.M.Koltun, Optics and Metrology of Solar Cells, Nauka, Moscow (1979) [in Russian].
18. H.R.Philipp, E.A.Taft, *Phys. Rev.*, **120**, 37 (1960).
19. Encyclopedia of Laser Physics and Technology, http://www.rp- photonics.com/encyclopedia_new.html.
20. Rutile, Optical Grade TiO_2 Single Crystal, http://www.mticrystal.com.
21. D.E.Morton, Characterizing Optical Thin films (II), http://www.dentonvacuum.com/n-paper.
22. V.M.Zolotarev, V.N.Morozov, E.V.Smirnova, Optical Constants of Natural and Technical Environments: A Reference Book, Khimia, Leningrad (1984) [in Russian].
23. S.V.Gils, Th. Dimogerontakis, G.Buytaert et al., *J. Appl. Phys.*, **98**, 083505-1 (2005), http://dx.doi.org/10.1063/1.20853.15.

Оптимізація тильно-поверхневого рефлектора тонких монокристалічних кремнієвих фотоелектричних перетворювачів

В.Р.Копач, М.В.Кіріченко, С.В.Шрамко, Р.В.Зайцев, І.Т.Тимчук, В.А.Антонова, О.М.Лістратенко

Показано, що для монокристалічних кремнієвих фотоелектричних перетворювачів (Si-ФЕП) сонячної енергії з товщиною базових кристалів 180–200 мкм оптимальним є тильно-поверхневий рефлектор TiO_2/Al з товщиною оксидного шару 0,18 мкм. Коефіцієнт відбиття зазначеним рефлектором фотоелектрично активного сонячного випромінювання, яке досягає тильної поверхні таких Si-ФЕП, при довжинах хвиль 0,88–1,11 мкм становить 81–92 % на відміну від 71÷87 % при безпосередньому контакті Al з тильною поверхнею базового кристала кремнію.